Available online at www.sciencedirect.com
SCIENCE DIRECT®
Journal of the European Ceramic Society 25 (2005) 1005–1013
www.elsevier.com/locate/jeurceramsoc

Phase formation in porous liquid phase sintered silicon carbide: Part III: Interaction between Al_2O_3–Y_2O_3 and SiC

J. Ihle*, M. Herrmann, J. Adler

Fraunhofer-Institute for Ceramic Technologies and Sintered Materials, Winterbergstr. 28, 01277 Dresden, Germany

Received 10 December 2003; received in revised form 6 April 2004; accepted 22 April 2004
Available online 17 July 2004

Abstract

The structure and phase formation of porous liquid phase sintered silicon carbide (porous LPS-SiC), containing yttria and alumina additives have been studied. The present paper is focused on the system Y–Al–Si–C–O. The systems Al–Si–C–O and Y–Si–C–O have been studied in previous papers [J. Eur. Ceram. Soc. (in press) parts I and II].

The reaction products of the interaction of Al_2O_3/Y_2O_3 with SiC and resulting microstructures were analysed by model experiments. The influences of different sintering atmospheres, namely argon and Ar/CO and different temperatures have been investigated. Thermodynamic calculations and sintering experiments reveal that silicides or carbides can be formed in addition to stable oxides. The main parameters controlling the formation of the different reaction products are the free carbon content, the oxygen activity and the temperature.

Using CO containing atmospheres, the decomposition of the oxide additives can be effectively suppressed and stable porous LPS-SiC can be produced.

Keywords: SiC; Liquid phase sintering; Phase development; Additives

1. Introduction

Silicon carbide is a prevalent ceramic material for many applications in harsh environmental conditions because of its resistance against high temperatures, aggressive chemicals and abrasion.[3] The sintering of SiC (S-SiC) is usually performed at very high temperatures up to 2200 °C with small amounts of boron and carbon, boron, or aluminium and carbon. In the case of LPS-SiC there is a liquid phase formation, due to the presence of Al_2O_3 and Y_2O_3 or other rare earth oxide additions, which subsequently accelerates the sintering in comparison to S–SiC. As a result, the sintering temperature can be decreased to 1800–2000 °C if the composition of the additives is close to the eutectic.[4,5]

The excellent properties of SiC promote its use in the filtration of abrasive suspensions as well as in acids. A high amount of open porosity, narrow pore size distribution and an adjustable pore size are an advantage for filtration applications of porous LPS-SiC.[6,7] Open porosities of up to 45% can be achieved in such a system, and pore sizes between 1 and 50 μm are possible.[7] Fig. 1 shows schematically the structure of porous LPS-SiC.[8]

The sintering process in combination with the formation of a liquid phase has an essential influence on structure, phase composition and subsequently the properties of the materials. The properties of LPS-SiC have been investigated and published by several authors.[4,5,9–15] In addition to the formation of yttrium–aluminium–garnet (YAG) as an intergranular phase between the SiC-grains, a reduction of the oxides by the silicon carbide can occur. Gas producing reactions between the oxides and the silicon carbide are associated with mass loss.

The decomposition of SiC during sintering with additions of Al_2O_3 and Al_2O_3/Y_2O_3 mixtures have been analysed by numerous authors.[1,2,4,10,11] The major weight loss in the SiC–Al_2O_3–Y_2O_3 system during sintering is a result of the formation of CO, SiO, Al_2O and Al. The sintering conditions influence the composition of the gas phase and consequently the extent of weight losses.[1,2,4,10,11] It is a common practice to implement a powder bed for minimising the mass loss by gas forming reactions during the sintering of LPS-SiC.

* Corresponding author. Tel.: +49 351 2553 682; fax: +49 351 2554 128.
E-mail address: Jan.Ihle@ikts.fraunhofer.de (J. Ihle).

0955-2219/$ – see front matter.
doi:10.1016/j.jeurceramsoc.2004.04.017

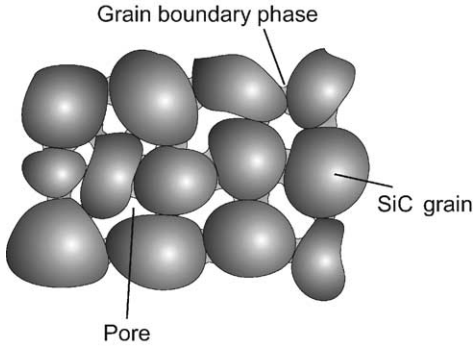

Fig. 1. Schematic view of the microstructure of porous LPS-SiC.[8]

In most cases a mixture of SiC and Al_2O_3 are used for the powder bed.[5,9,11,16]

The systems Si–C–Al–O and Si–C–Y–O were analysed by model experiments and thermodynamic calculations, and were presented in previous papers.[1,2] Different degrees of decomposition reactions and structures at various temperatures and atmospheres were observed. Samples consisting of 50 wt.% SiC and 50 wt.% Al_2O_3, sintered in argon at 2223 K (1950 °C) contained SiC and additionally elemental silicon and aluminium after sintering. These results are in accordance with Misra[17] and Mulla et al.[18] however the formation of such phases was found at even lower temperatures. The products of the SiC/Al_2O_3 decomposition depend on the free carbon content in the system.[1]

Mulla et al.[18] reported that the reaction between SiC and Al_2O_3 during sintering can be reduced if a pure CO gas atmosphere is used. Our results, presented in a previous paper,[1] showed that the decomposition can be successfully suppressed even if a low CO partial pressure is used in the Ar atmosphere.

Baud et al.[11] described the decomposition of a SiC–Al_2O_3/Y_2O_3 mixture as being similar to that of a pure SiC–Al_2O_3 mixture. Thermodynamic calculations reveal that gaseous CO, SiO, Al_2O and Al are the main species present in the sintering atmosphere in both additive systems.[11]

Cordrey et al.[9] investigated the sintering behaviour of silicon carbide with 2 and 5 wt.% yttrium oxide additive. On the basis of an EDS and XRD analysis they assumed that a Al–Y–C–O compound and a Y–C–O compound may have formed. Using EDX, van Dijen and Mayer[19] found a mixed carbide phase Y–Al–O–C and a mixed Y–Al–Si–O oxide phase with unknown composition, in addition to the usual YAG, in the secondary phase, after sintering in an argon atmosphere at 1900 °C. Grande et al.[4] and Nagano et al.[20] describe a decomposition reaction of Y_2O_3. They did not measure a significantly reduced yttrium content in the secondary phase in LPS-SiC samples. Model experiments in the system Si–Y–C–O have shown that depending on the conditions beside silicon carbide and yttrium oxide, silicides or yttrium containing carbides (mainly $Y_3Si_2C_2$, YC_2) can occur, resulting in a degradation of samples during exposure to air after sintering.[2] Thermodynamic calculations of the system Si–Y–C–O–Ar have shown that CO is the main component of the gas phase beside Ar.[2] Therefore, the decomposition reaction between SiC and Y_2O_3 during sintering can be suppressed successfully if a CO partial pressure in an Ar/CO atmosphere is used.[2]

The data show that no reliable information about the changes of the phase composition with changing atmosphere and carbon content is available for the interaction of SiC with Al_2O_3/Y_2O_3 additions. This information is required for the reproducible preparation of porous LPS-SiC because the interactions with the gas phase in these materials are more intensive than for dense materials due to the high open porosity and associated high sample surface area during the sintering process.

Consequently, in the present paper we seek to summarise an experimental study and thermodynamic calculations of the temperature, carbon content and gas atmosphere dependence of phase formation in the system Si–Al–Y–C–O.

2. Experimental

Samples with a higher oxide content than in the original compositions of porous LPS-SiC were produced to enable a better detection of minor phases and thereby facilitating an improvement in the understanding of phase formation. A composition of 50 wt.% α-SiC (ESK F1200 green) and 50 wt.% additive was chosen. The additive consisted of 64.4 wt.% Al_2O_3 (Alcoa A16 SG) and 35.6 wt.% Y_2O_3 (H.C. Starck grade C). The samples were formed into tablets with a thickness of 5 mm and a diameter of 25 mm. All samples were sintered at 1 bar gas pressure in a graphite furnace. The sintering conditions are shown in Table 1.

Graphite crucibles were used for the sintering of samples. Graphite foil was placed between crucibles and the samples in order to prevent an adhesion of the samples to the base of the crucible due to liquid formation during sintering. It was not possible to accurately measure the post sintering mass loss because some graphite foil was bonded to the samples after sintering. No mass loss results are therefore presented.

The phase composition of the samples was determined by X-ray diffraction analysis (XRD 7; Seifert-FPM; Cu Kα) and using JCPDS standards.[21] The microstructures of polished surfaces were examined using optical microscopy and scanning electron microscopy with attached EDX (Leica Stereoscan 260).

The FactSage® software package was used for thermodynamic calculations.[22] The partial pressure of gas phases and phase formation in the system Al–Y–Si–C–O–Ar were calculated. The necessary thermodynamic data for calculations were taken from the SGTE (Scientific Group Thermodata Europe) pure substance database (SGPS)[23] and solution database (SGSL)[24] as well as the special data set of the system Y–Al–Si–C–O from SGTE[25] based on the data set of Groebner.[26] As in Part 1[1] the data for the system Al–O–C

Table 1
Sintering temperatures, dwell time, atmospheres and phase composition

Temperature (°C)	Dwell time (h)	Atmosphere	Phase composition of sintered samples
1850	1	Argon	α-SiC, $Y_3Al_5O_{12}$, Al_2O_3
1925	1	Argon	α-SiC, $Y_3Al_5O_{12}$, YAl_2Si_2, Si, Al
1925	1	Argon + CO	α-SiC, $Y_3Al_5O_{12}$, Al_2O_3
1950	1	Argon	α-SiC, $Y_3Al_5O_{12}$, $YAlO_3$, YAl_3C_3

Table 2
Thermodynamically calculated phase compositions of a mixture of 14.8 mol SiC + 2.5 mol Al_2O_3 + 1.5 mol Y_2O_3 with different carbon content and different amount of argon at 2223 K (1950 °C)

Phases	Argon (mol) (C = 0.001 mol)			Argon (mol) (C = 1 mol)			Argon (mol) (CO = 0.1 mol)		
	0.1	1	10	0.1	1	10	0.1	1	10
SiC (mol)	14.66	14.51	13.21	14.78	14.71	14.04	14.75	14.61	13.30
C (mol)	–	–	–	0.553	–	–	–	–	–
Al_4SiC_4 (mol)	–	–	–	0.011	0.067	–	–	–	–
Oxide melt (mol)	3.983	3.906	3.338	4.095	3.924	3.372	4.027	3.944	3.367
Liquid metal (mol)	0.157	0.370	2.188	–	–	1.316	–	0.204	2.030
Al (mole fraction)	0.444	0.418	0.357	–	–	0.486	–	0.431	0.359
Al (activity)	0.386	0.364	0.330	–	–	0.449	–	0.375	0.331
C (mole fraction)	0.020	0.019	0.019	–	–	0.035	–	0.019	0.019
C (activity)	0.011	0.011	0.010	–	–	0.014	–	0.011	0.010
Si (mole fraction)	0.506	0.529	0.570	–	–	0.432	–	0.517	0.569
Si (activity)	0.401	0.421	0.432	–	–	0.311	–	0.411	0.432
Y (mole fraction)	0.030	0.034	0.054	–	–	0.047	–	0.032	0.053
Y (activity)	2E−5	2E−5	3E−5	–	–	5E−5	–	2E−5	3E−5
Ar (bar)	0.799	0.804	0.830	0.579	0.635	0.822	0.786	0.802	0.829
CO (bar)	0.144	0.140	0.122	0.374	0.317	0.130	0.159	0.142	0.122
SiO (bar)	0.023	0.024	0.022	0.006	0.006	0.012	0.021	0.023	0.022
Al_2O (bar)	0.016	0.015	0.011	0.020	0.020	0.016	0.017	0.016	0.011
Al (bar)	0.017	0.016	0.015	0.020	0.021	0.020	0.017	0.016	0.015

Table 3
Thermodynamically calculated phase compositions of a mixture of 15.8 mol SiC + 4 mol Al_2O_3 + 1 mol Y_2O_3 with different carbon content and different amount of argon at 2223 K (1950 °C)

Phases	Argon (mol) (C = 0.001 mol)			Argon (mol) (C = 1 mol)			Argon (mol) (CO = 0.1 mol)		
	0.1	1	10	0.1	1	10	0.1	1	10
SiC (mol)	15.65	15.39	13.13	15.77	15.71	13.99	15.75	15.49	13.22
C (mol)	–	–	–	0.284	–	–	–	–	–
Al_4SiC_4 (mol)	–	–	–	0.024	0.053	–	–	–	–
Oxide melt (mol)	4.989	4.880	3.874	5.101	4.884	3.881	5.024	4.914	3.903
Liquid metal (mol)	0.171	0.531	3.660	–	0.040	2.793	0.003	0.364	3.507
Al (mole fraction)	0.400	0.416	0.421	–	0.678	0.491	0.403	0.420	0.422
Al (activity)	0.303	0.319	0.331	–	0.613	0.402	0.306	0.323	0.332
C (mole fraction)	0.011	0.012	0.013	–	0.055	0.018	0.011	0.012	0.013
C (activity)	0.009	0.009	0.009	–	0.023	0.011	0.009	0.009	0.009
Si (mole fraction)	0.583	0.566	0.556	–	0.264	0.484	0.579	0.562	0.555
Si (activity)	0.523	0.506	0.488	–	0.196	0.408	0.523	0.502	0.487
Y (mole fraction)	0.006	0.006	0.010	–	0.003	0.008	0.006	0.006	0.010
Y (activity)	1E−6	2E−6	3E−6	–	3E−6	4E−6	1E−6	2E−6	3E−6
Ar (bar)	0.710	0.713	0.737	0.348	0.584	0.732	0.710	0.713	0.736
CO (bar)	0.203	0.202	0.186	0.589	0.330	0.194	0.203	0.202	0.186
SiO (bar)	0.055	0.051	0.043	0.010	0.012	0.032	0.055	0.050	0.043
Al_2O (bar)	0.019	0.020	0.019	0.032	0.047	0.025	0.019	0.020	0.019
Al (bar)	0.013	0.014	0.015	0.020	0.027	0.018	0.013	0.014	0.015

were also taken from Lihrmann et al.[27] in accordance with Qiu and Metselaar[28] and Yokokawa et al.[29]

3. Results and discussion

3.1. Thermodynamic calculations

The calculations indicate the presence of different compositions depending on the amount of C, the CO activity and the amount of argon used in the calculations. The composition also varies with the degree of Al_2O_3 content. Table 2 shows the composition of the mixture of 50 wt.% SiC and 50 wt.% additive at 2223 K with a different carbon content on the one hand and with 0.1 mol CO on the other hand if the mol ratio Al_2O_3:Y_2O_3 is 5:3. Table 3 shows by comparison the composition of the mixture if a mol ratio of 4 Al_2O_3:1 Y_2O_3 is used for the additive. In the calculations (Tables 2 and 3) beside the oxide melt an additional liquid metallic phase was observed under different conditions. The composition and amount of the liquid metal changes with increasing amount of carbon in the system. The calculations showed that the liquid metal formation depends most strongly on gas volume, carbon content and CO content of the starting composition.

The calculations using different additive compositions (Tables 2 and 3) have shown that with increasing amount of Al_2O_3 the partial pressure of the evolved gases increases, most notably that of CO and Al_2O. These results showed that along with the carbon content, the amount of Al_2O_3 in the system is important for the phase formation. Further calculations were therefore performed assuming a high alumina content. The given amounts, according to a mixture of 50 wt.% SiC and 50 wt.% additive, were 15.8 mol SiC, 4 mol Al_2O_3, 1 mol Y_2O_3 and 1 mol argon. The corresponding composition of additive was consistent with a mol ratio Al_2O_3:Y_2O_3 of 4:1. This starting composition was altered in the direction of a deficit of carbon in comparison to the stoichiometry of the SiC and in the direction of a content of up to 0.5 mol free carbon. This was necessary because the amount of carbon available during sintering can not be easily predicted.

The calculations (Fig. 2) showed that the main gas species of the system in the temperature range 1950–2250 K are Ar, CO, SiO, Al_2O and Al. Their partial pressures as a function of carbon content and temperature are plotted in Fig. 3. All other gas species have a partial pressure which is several orders of magnitude lower (Fig. 2). Gaseous Al has a maximum partial pressure of 0.025 bar at 2250 K (calculations with 0.5 mol added carbon) which is nearly half of that of Al_2O under same conditions. The gas pressure of gaseous Si is less than 0.0002 bar (maximum under the calculated conditions) and the pressures for the other compounds such as AlO, Y, YO, Y_2O, etc. are lower than 10^{-5} bar. The calculated partial pressure of SiO is higher than the partial pressure of CO up to a temperature of

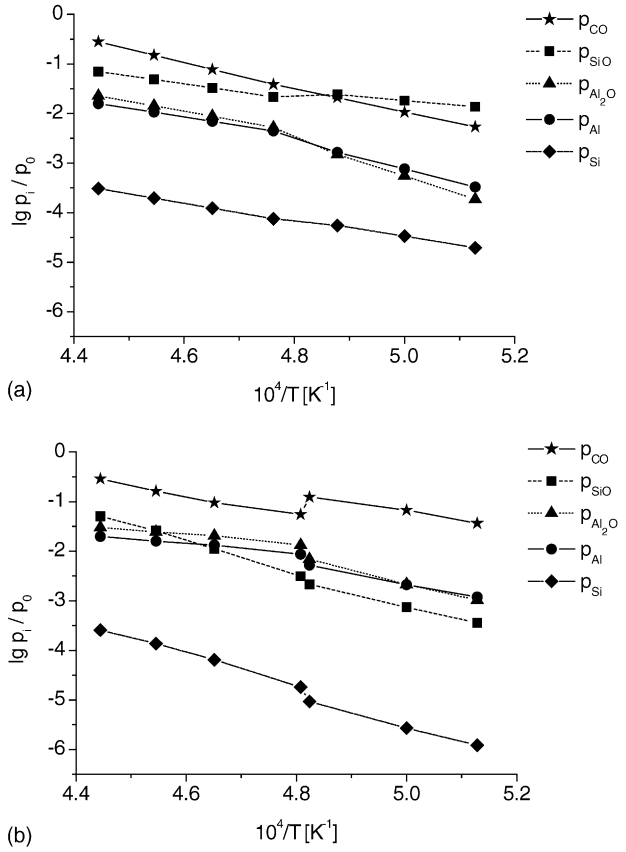

Fig. 2. Calculated partial pressures of gas species of the system Si–Y–Al–C–O–Ar as a function of the inverse temperature (p_0 = 0.1 MPa). The Ar pressure is the residual to 0.1 MPa and not shown in the graphs. (a) Results of calculations with deficit of −0.1 mol carbon (condensed phases: SiC, liquid metal, oxide melt for $10^4/T \leq 4.76\,K^{-1}$; SiC, YAG, liquid metal, oxide melt for $10^4/T \leq 4.79\,K^{-1}$; SiC, YAG, Al_2O_3, liquid metal, oxide melt for $10^4/T \leq 4.80\,K^{-1}$; above SiC, YAG, Al_2O_3, liquid metal). (b) Results of calculations with 0.2 mol added carbon (condensed phases: SiC, liquid metal, oxide melt for $10^4/T \leq 4.76\,K^{-1}$; SiC, YAG, liquid metal, oxide melt for $10^4/T \leq 4.77\,K^{-1}$; SiC, YAG, Al_4SiC_4, liquid metal, oxide melt for $10^4/T \leq 4.78\,K^{-1}$; SiC, YAG, Al_4SiC_4, oxide melt for $10^4/T \leq 4.81\,K^{-1}$; SiC, YAG, Al_2O_3, Al_4SiC_4, oxide melt for $10^4/T \leq 4.82\,K^{-1}$; SiC, YAG, Al_2O_3, Al_4SiC_4 for $10^4/T \leq 4.87\,K^{-1}$; above SiC, YAG, Al_2O_3, Al_4SiC_4, C).

2050 K in the case of a carbon deficiency but much lower than the CO partial pressure if a higher carbon activity is assumed (Fig. 2). With increasing carbon content the partial pressure of Al_2O rises and the partial pressure of SiO decreases.

The existence of a liquid metal C–Al–Y–Si was indicated under these conditions in a temperature range of 1950–2250 K, and its formation depends on the carbon content. In the absence of excess carbon liquid metal formation may occur at temperatures as low as 1950 K. The temperature of formation increases with increasing carbon content and with 0.5 mol additional carbon the liquid metal phase may only form above 2173 K. In the calculations the Al_2O_3 is stable up to approximately 2070 K. Therefore the partial pressures of Al, Al_2O are very similar to the

pressures observed for the interaction of Al_2O_3 and SiC up to this temperature.[1]

In case of the calculations with an additive mol ratio corresponding to the composition of YAG the main gas species that form are the same as in the calculation using an excess of Al_2O_3, but it was seen that the CO partial pressure decreased from 0.324 to 0.259 bar at 2250 K. The partial pressures of SiO and Al_2O were also seen to be lower (compare also Tables 2 and 3).

The calculated compositions of the gas phase and the liquid metal reveal the following simplified decomposition reaction as the most probable at temperatures higher than

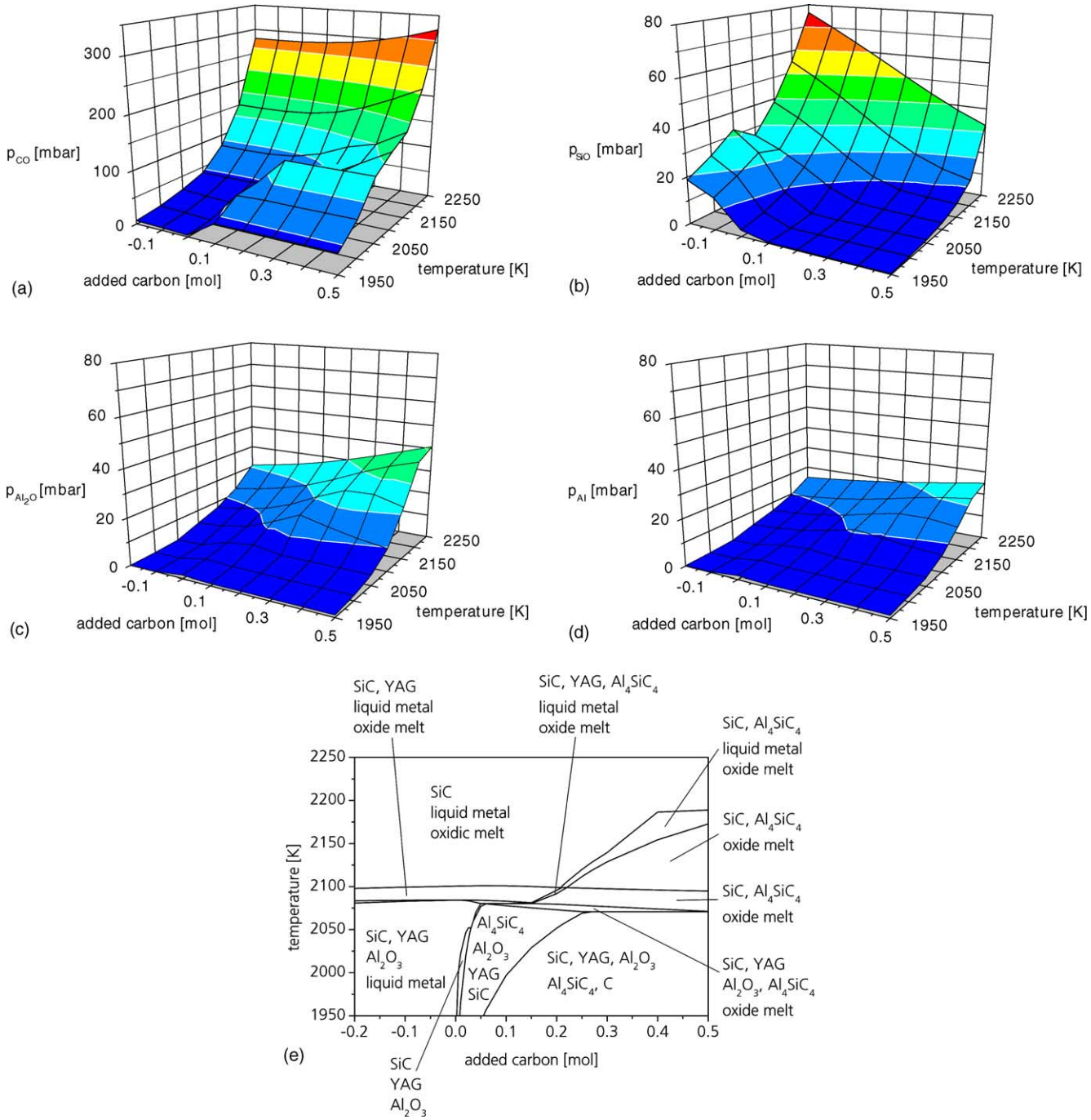

Fig. 3. Results of thermodynamic calculations of partial pressures as a function of carbon content and temperature in the system Y–Al–Si–C–O–Ar (initial composition: 15.8 mol SiC, 4 mol Al_2O_3, 1 mol Y_2O_3, 0.2, . . . , 0.5 mol C, 1 mol Ar). (Different grey levels are only used for better visualisation of the partial pressure.) (a) Partial pressure of CO; (b) partial pressure of SiO; (c) partial pressure of Al_2O; (d) partial pressure of Al; (e) calculated condensed phases (the arrow marks the stoichiometric composition).

1950–2150 K in the system $SiC–Al_2O_3–Y_2O_3$:

$$4SiC\,(s) + 2Al_2O_3\,(s, l) \rightarrow 4CO\,(g) + SiO\,(g) + Al_2O\,(g) + 0.5Al\,(g) + 3Si\,(l) + 1.5Al\,(l) \quad (1)$$

The formation of the metallic melt strongly depends on the excess of carbon (Fig. 3e). The melt in this system is Si–Al rich and can contain some yttrium and carbon (see Tables 2 and 3).

At lower temperatures and in the presence of free carbon the formation of Si–Al containing carbides dominates over the formation of the metallic melt.

These reactions are very similar to the findings for the interaction in the pure Al_2O_3–SiC mixture. The partial pressure of the CO at sintering temperatures in the presence of carbon, which can be safely assumed due to the presence of the graphite crucible, heater and insulation in the sintering furnace, is much higher than the other species. The samples therefore suffer mainly from a loss of oxygen and to a lesser degree Al and Si losses.

The compositions of the anticipated condensed phases reveal that there is only a small area were no metallic melt or carbide is formed during sintering in pure argon. On the other hand, by adding CO the decomposition can be prevented (Tables 2 and 3), i.e. by using CO partial pressures higher than those calculated in the Ar atmosphere (Fig. 3) decomposition can be prevented.

In the thermodynamic calculations the SiO_2 existing on the surface of the SiC-starting powder was not taken into account. From previous investigations it is known that it evaporates nearly completely between 1750 and 1950 K, i.e. below the temperature range considered in the calculations discussed here.

The thermodynamically determined phase relations were proved with the aid of model experiments.

3.2. Experimental determination of the interaction

As shown in Table 1, different condensed phases were observed depending on the sintering conditions. Samples sintered at 1850 °C consisted of α-SiC, YAG and a small amount of Al_2O_3, whereas the phase composition of the samples sintered at 1925 and 1950 °C were completely different.

In samples sintered in Ar at 1925 °C YAl_2Si_2 as well as Si and Al were detected, and Al_2O_3 completely disappeared (Fig. 4). The powder diffraction file (PDF) of the phase YAl_2Si_2 is not available in the JCPDF,[21] and therefore the diffraction pattern was taken from Groebner.[26] YAl_2Si_2 was not a major phase in samples sintered at 1925 °C. It can be assumed that YAl_2Si_2 precipitates from the metallic melt during cooling in a similar way to Al and Si.

At 1950 °C in addition to YAG and SiC, there was a formation of $YAlO_3$ and YAl_3C_3 (Fig. 5). The powder diffraction file (PDF) of the phase YAl_3C_3 was not available in the JCPDF,[21] and so the diffraction pattern was also taken from Groebner.[26]

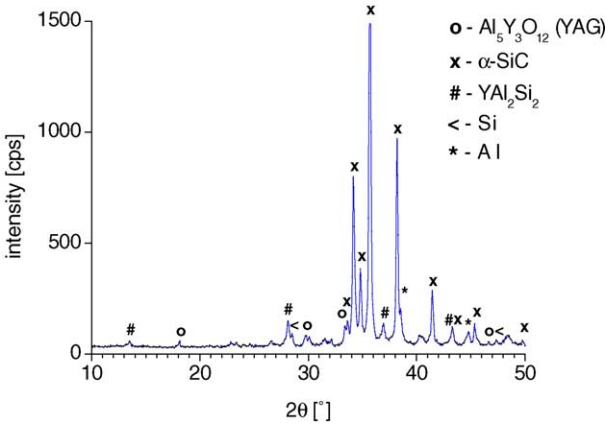

Fig. 4. Result of X-ray diffraction analysis of samples sintered in argon at 2198 K (1925 °C).

Some samples sintered at 1925 or 1950 °C decomposed to powder after several weeks storage in air at room temperature. In other cases, samples sintered under the same nominal conditions showed destruction already after a few hours. The same result was found for porous LPS-SiC with a lower additive content. Fig. 6 shows the decomposed regions of these porous LPS-SiC samples. Beside α-SiC and YAG, $YAlO_3$ or $Y_4Al_2O_9$ no further phases in the samples with low additive content were detectable by XRD. Mass spectrometric measurements (Fig. 7) of porous LPS-SiC samples in humid atmosphere had shown that C_2H_2 was formed (mass number m26 was observed together with the mass number m18 for H_2O).[8] According to Kost et al.[30] this is an evidence of the decomposition of YC_2. Other yttrium carbides like YC, Y_2C_3 show a similar behaviour and decompose in water very quickly in a few minutes.[30,31] The formation of YC_2 under such conditions was shown in samples with starting compositions containing only Y_2O_3 and SiC.[2]

Hence it is assumed that the formation of an yttrium containing carbide occurs during the sintering of porous

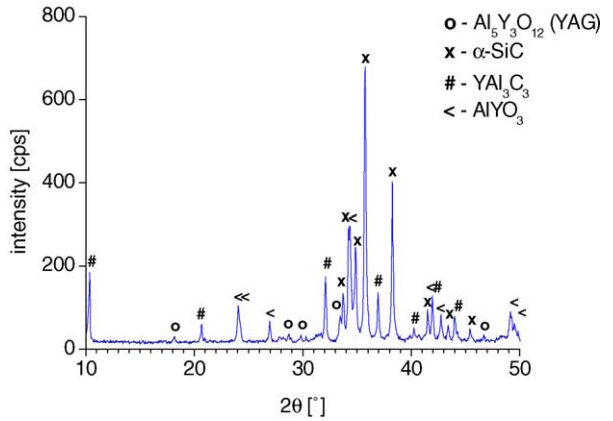

Fig. 5. Result of X-ray diffraction analysis of samples sintered in argon at 2223 K (1950 °C).

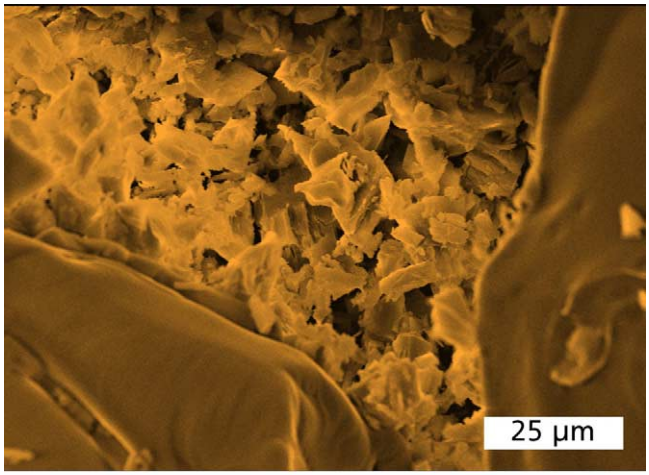

(a)

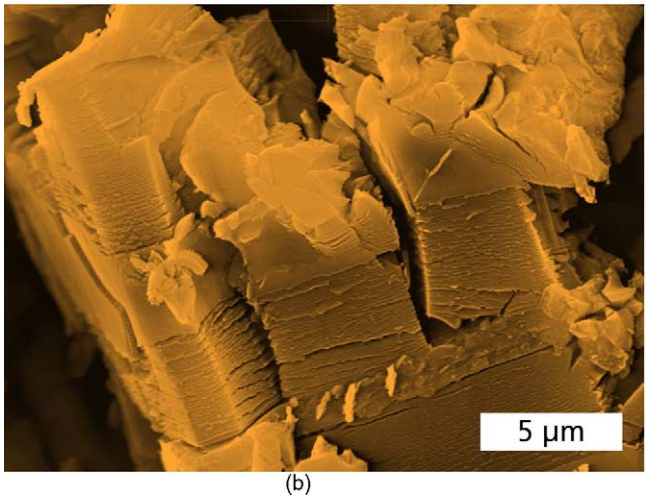

(b)

Fig. 6. Micrographs of destructed regions of sintered porous LPS-SiC samples during exposure in air. (a) Destructed secondary phase between the SiC grains; (b) destructed particle of the secondary phase.

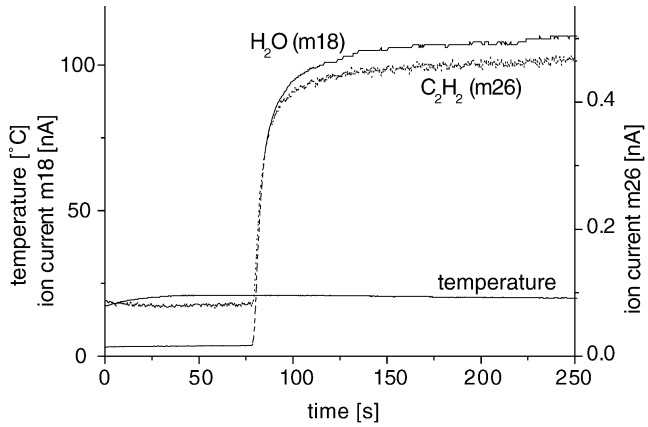

Fig. 7. Result of mass spectrometric measurement of porous LPS-SiC sample in a humid atmosphere.[8]

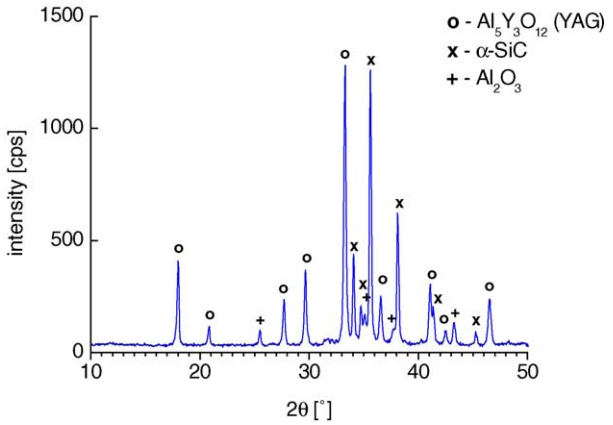

Fig. 8. Result of X-ray diffraction analysis of samples sintered in argon + CO at 2198 K (1925 °C).

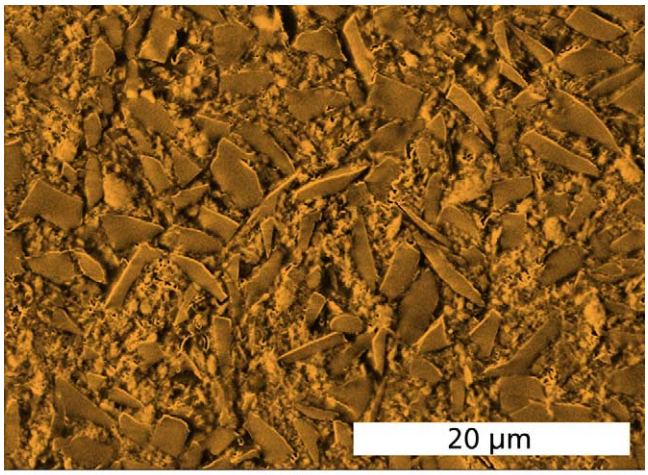

(a)

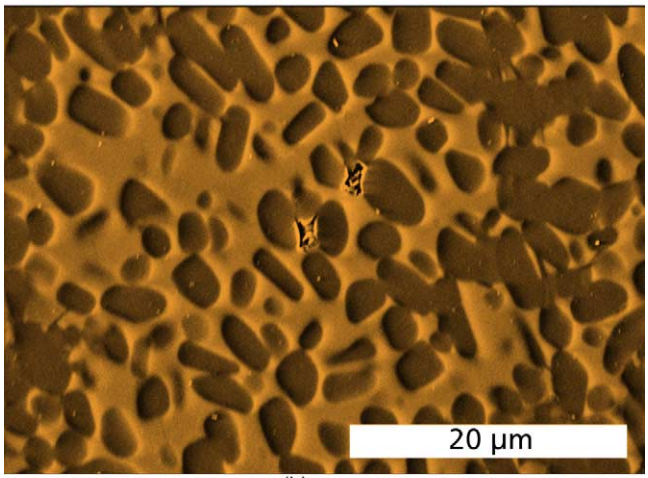

(b)

Fig. 9. Optical micrographs of sintered samples (polished cross sections). (a) Sample sintered in pure argon atmosphere (commencing destruction); (b) sample sintered in Ar/CO atmosphere.

LPS-SiC in Ar, at least in small amounts. The thermodynamic calculations indicate that YC_2 can be formed only in materials where the Al_2O_3 is completely evaporated. This could be the case in the near surface region of the samples. Especially in samples with low additive content and with some residual carbon in the composition, an intensive decomposition in the near surface region can be take place resulting in the depletion of Al_2O_3, thereby resulting in the formation of some YC_2. An indication of this behaviour is evident from the strong shift of the composition towards Y–Al carbides during sintering at 1950 °C in argon.

Based on the thermodynamic considerations and previous results of the investigation of the interaction of SiC and Al_2O_3,[1] and SiC and Y_2O_3[2] it can be concluded that sintering in a CO containing atmosphere should prevent these decompositions. The calculated minimum required CO partial pressure for stabilising the system SiC–Al_2O_3–Y_2O_3 was applied (Fig. 3a). The results show that a stabilisation of SiC and the secondary phase consisting of YAG and Al_2O_3 was achieved when a mixed atmosphere of argon and CO was used. The samples sintered at 1925 °C in this mixed atmosphere at 1 bar consist only of SiC, YAG and Al_2O_3 after sintering (Table 1; Fig. 8).

The different phase compositions also result in different microstructures (Fig. 9). The secondary phases of samples sintered in a pure argon atmosphere are separated from the SiC grains and subsequently lead to the complete destruction of the samples (Fig. 9a). Samples sintered in a mixed atmosphere show rounded SiC grains embedded in the secondary phase indicating their conversion during sintering (Fig. 9b). Because of the high amount of additives there is a low degree of open porosity in the samples for the model experiments, i.e. the structure is similar to the microstructure of dense material with a high additive content. The model material, however, clearly illustrated the stability or non stability of that particular composition with regards to the sintering conditions.

4. Conclusions

Model experiments for the investigation of the interaction of Y_2O_3, Al_2O_3 and SiC were performed and compared with thermodynamic calculations.

Thermodynamic calculations showed that the phase formation strongly depends on the content of free carbon in the system, the sintering temperature and oxygen activity. Without additional carbon in the system the existence of a Si–Al rich liquid metal (C–Al–Y–Si) in a temperature range of 1950–2250 K was predicted. According to the thermodynamic calculations, an increasing amount of free carbon increases the temperature of the formation of the liquid metal and favours the formation of mixed carbides. CO is the main gas species formed during interaction of Y_2O_3, Al_2O_3 and SiC. All other gas species that are formed are at least one order of magnitude lower in partial pressure.

Calculated decomposition of the oxide phases during sintering was confirmed in sintering experiments.

Beside the silicon carbide and oxides, silicides or yttrium containing carbides were formed. The reason for the sporadic destruction of samples lies in the decomposition of the yttrium containing carbides formed during sintering in argon.

Experiments with CO containing Ar-atmospheres have shown that a stabilisation of SiC and the secondary oxide phase can be achieved. The samples sintered at 1925 °C in the mixed atmosphere consisted of only SiC, YAG and Al_2O_3 after sintering.

Contrary to samples sintered in pure argon, samples sintered in the mixed atmosphere show a homogeneous microstructure and exhibit no destruction in water or humid atmospheres. Using CO containing sintering atmospheres the decomposition of the oxide additives of the porous LPS-SiC can be effectively suppressed and stable materials can consequently be produced.

References

1. Ihle, J., Herrmann, M. and Adler, J., Phase formation in porous liquid phase sintered silicon carbide: I. Interaction between Al_2O_3 and SiC. *J. Eur. Ceram. Soc.* 2005, **25**, 987–995.
2. Ihle, J., Herrmann, M. and Adler, J., Phase formation in porous liquid phase sintered silicon carbide: II. Interaction between Y_2O_3 and SiC. *J. Eur. Ceram. Soc.* 2005, **25**, 997–1003.
3. Schwetz, K. A., Silicon carbide-based hard materials. In *Handbook of Ceramic Hard Materials*, ed. R. Riedel. Wiley-VCH, Germany, 2000.
4. Grande, T., Sommerset, H., Hagen, E., Wiik, K. and Einarsrud, M.-A., Effect of weight loss on liquid-phase-sintered silicon carbide. *J. Am. Ceram. Soc.* 1997, **80**(4), 1047–1052.
5. Baud, S., Thévenot, F. and Chatillon, C., High temperature sintering of SiC with oxide additives: IV. Powder beds and the influence of vaporization on the behaviour of SiC compacts. *J. Eur. Ceram. Soc.* 2003, **23**, 29–36.
6. Schubert, C., Adler, J., Schulz, I. and Klose, T., Ceramic membranes with high physical and chemical stability based on SiC and Si_3N_4. In *Conference on Materials Research Under Environmental Aspects, Dresden 1994*. Environmental Aspects in Materials Research, Warlington, H. (pub), 1994, p. 283.
7. Adler, J., Klose, T. and Piwonski, M., *SiC Ceramics with Pore Sizes from Nanometers to Micrometers, Materials Week 1998, Band III*. Wiley-VCH, 1999, pp. 287–292.
8. Ihle, J., *Structure and Properties of Porous Liquid Phase Sintered Silicon Carbide Ceramics*. Diploma thesis, Fraunhofer Institute for Ceramic Technologies and Sintered Materials, Freiberg University of Mining and Technology, 2000.
9. Cordrey, L., Niesz, D. E. and Shanefield, D. J., Sintering of silicon carbide with rare-earth oxide additions. In *Sintering of Advanced Ceramics*, ed. C. A. Handwerker, J. E. Blendell and W. Kayser. The American Ceramic Society, Inc., Westerville, OH, 1990, pp. 618–636.
10. Schuesselbauer, E., Adler, J., Jaenicke-Roeßler, K. and Leitner, G., *Sintering Investigations on LPS-SiC, Werkstoffwoche 98, Band VII*. 1999, pp. 207–212.
11. Baud, S., Thévenot, F., Pisch, A. and Chatillon, C., High temperature sintering of SiC with oxide additives: I. Analysis in the SiC–Al_2O_3 and SiC–Al_2O_3–Y_2O_3 systems. *J. Eur. Ceram. Soc.* 2003, **23**, 1–8.
12. Falk, L. K. L., Microstructural development during liquid phase sintering of silicon carbide ceramics. *J. Eur. Ceram. Soc.* 1997, **17**, 983–994.

13. Samanta, A. K., Dharguupta, K. K. and Ghatak, S., Decomposition reactions in the SiC–Al–Y–O system during gas pressure sintering. *Ceram. Int.* 2001, **27**, 123–133.
14. She, J. H. and Ueno, K., Effect of additive content on liquid-phase sintering on silicon carbide. *Mater. Res. Bull.* 1999, **34**(10/11), 1629–1636.
15. Pujar, V. V., Jensen, R. P. and Padture, N. P., Densification of liquid-phase-sintered silicon carbide. *J. Mater. Sci. Lett.* 2000, **19**, 1011–1014.
16. Winn, E. J. and Clegg, W. J., Role of the powder bed in the densification of silicon carbide sintered with yttria and alumina additives. *J. Am. Ceram. Soc.* 1999, **82**(12), 3466–3470.
17. Misra, A. K., Thermochemical analysis of the silicon-carbide-alumina reaction with reference to liquid phase sintering of silicon carbide. *J. Am. Ceram. Soc.* 1991, **74**(2), 345–351.
18. Mulla, M. A., Krstic, V. D. and Thompson, W. T., Reaction-inhibition during sintering of SiC with Al_2O_3 additions. *Can. Metall. Q.* 1995, **34**(4), 357–362.
19. van Dijen, F. K. and Mayer, E., Liquid phase sintering of silicon carbide. *J. Eur. Ceram. Soc.* 1996, **16**, 413–420.
20. Nagano, T., Kaneko, K., Zhan, G.-D. and Mitomo, M., Effect of atmosphere on weight loss in sintered silicon carbide during heat treatment. *J. Am. Ceram. Soc.* 2000, **83**(11), 2781–2787.
21. *Joint Committee on Powder Diffraction Standards* (*JCPDS*), ASTM, Swartmore, 2001
22. Bale, C. W., Chartrand, P., Degterov, S. A., Eriksson, G., Hack, K., Ben Mahfoud, R. *et al.*, FactSage Thermochemical software and databases. *Calphad* 2002, **26**(2), 189–228.
23. *SGPS–SGTE Pure Substances Database*. Scientific Group Thermodata Europe, 2000.
24. *SGSL–SGTE Alloy Solutions Database*. Scientific Group Thermodata Europe, 1998.
25. *9288A00S–SGTE Si–Y–Al–C–O Database*. Scientific Group Thermodata Europe, 2000.
26. Groebner, J., *Constitution Calculations in the System Y–Al–Si–C–O*. Ph.D. thesis, University of Stuttgart, Germany, 1994.
27. Lihrmann, J. M., Tirlocq, J., Descamps, P. and Cambier, F., Thermodynamics of the Al–C–O system and properties of SiC–AlN–Al_2OC composites. *J. Eur. Ceram. Soc.* 1999, **19**, 2781–2787.
28. Qiu, C. and Metselaar, R., Phase relations in the aluminium carbide-aluminium nitride-aluminium oxide system. *J. Am. Ceram. Soc.* 1997, **80**(8), 2013–2020.
29. Yokokawa, H., Fujishige, M., Ujiie, S. and Dokiya, M., Phase relations associated with the aluminium blast furnace: aluminium oxycarbide melts and Al–C–X (X = Fe, Si) liquid alloys. *Metall. Trans. B* 1987, **18B**, 433–444.
30. Kost, M. E., Schilow, A. L., Michewa, W. I. *et al.*, *Chemistry of Rare Earth Compounds*. Nauka, Moscow, 1983, pp. 69–95.
31. *Gmelin Handbook of Inorganic and Organometallic Chemistry, 8th ed. Rare Earth Elements, C 12a, Compounds with Carbon*. Springer-Verlag, 1995.